

# Rapid Broad Spectrum Detection of Carbapenemases with a Dual Fluorogenic-Colorimetric Probe

Chi-Wang Ma, Kenneth King-Hei Ng, Bill Hin-Cheung Yam, Pak-Leung Ho, Richard Yi-Tsun Kao, and Dan Yang\*

Cite This: *J. Am. Chem. Soc.* 2021, 143, 6886–6894

Read Online

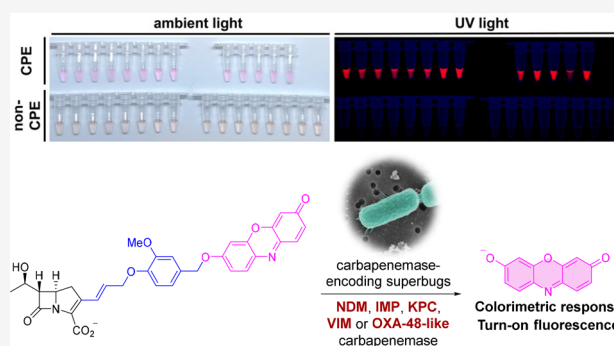
ACCESS |

Metrics & More

Article Recommendations

Supporting Information

**ABSTRACT:** Carbapenems stand as one of the last-resort antibiotics; however, their efficacy is threatened by the rising number and rapid spread of carbapenemases. Effective antimicrobial stewardship thus calls for rapid tests for these enzymes to aid appropriate prescription and infection control. Herein, we report the first effective pan-carbapenemase reporter **CARBA-H** with a broad scope covering all three Ambler classes. Using a chemical biology approach, we demonstrated that the absence of the  $1\beta$ -substituent in the carbapenem core is key to pan-carbapenemase recognition, which led to our rational design and probe development. **CARBA-H** provides a dual colorimetric-fluorogenic response upon carbapenemase-mediated hydrolysis. A clear visual readout can be obtained within 15 min when tested against a panel of carbapenemase-producing Enterobacteriaceae (CPE) clinical isolates that notably includes OXA-48 and OXA-181-producing strains. Furthermore, **CARBA-H** can be applied to the detection of carbapenemase activity in CPE-spiked urine samples.



## INTRODUCTION

Carbapenems are one of the most effective broad-spectrum drugs-of-last-resort against bacterial infection. However, the emergence and dissemination of resistance toward carbapenems in recent decades have become a major public health issue worldwide.<sup>1</sup> Microbial production of carbapenemases, enzymes that catalyze the hydrolytic degradation of carbapenems, in addition to virtually all other  $\beta$ -lactams, represents the most clinically important resistance mechanism in carbapenem-resistant bacteria.<sup>2</sup>

Carbapenemases belong to the larger family of  $\beta$ -lactamases and are categorized based on their amino acid sequences and hydrolysis mechanisms under the Ambler classification.<sup>2,3</sup> Carbapenemases in Classes A (e.g., KPC) and D (e.g., OXA-48-like) are serine hydrolases, and those in Class B (e.g., NDM, IMP, VIM) are Zn-dependent metallo- $\beta$ -lactamases. Over 200 unique carbapenemases have been identified to date, and the numbers are ever increasing.<sup>2</sup>

These carbapenemases are usually encoded on mobile genetic elements which greatly facilitate the transmission of the resistance, even across different bacterial species, through horizontal gene transfer.<sup>2</sup> Effective infection control programs are therefore key to curtail their spread in hospitals and dissemination into the community.<sup>1</sup> Patients infected by carbapenem-resistant bacteria may not show distinct symptoms, yet delay in effective treatment can lead to life-threatening complications like sepsis.<sup>4,5</sup> This poses a great

challenge for clinicians in choosing the appropriate antibiotics from the hierarchy of therapeutic options. Rapid identification of carbapenemases therefore provides the bedrock for both infection control and appropriate antibiotic prescription, two main pillars in antimicrobial stewardship.

Despite their sensitivity in detecting certain carbapenemase-encoding genes, genotypic tests generally suffer from high cost, labor-intensive protocols and requirement of specialized instrumentation.<sup>6</sup> Furthermore,  $\beta$ -lactamases within the OXA-family that exhibit diverse carbapenemase activities may not be readily distinguished by polymerase chain reaction (PCR). Immunochromatographic assays, including RESIST-4 and CARBA 5, which do not require sophisticated instruments, have also been developed.<sup>6</sup> However, the scope of these assays are delimited by recognizing particular fragment of DNA or protein sequence, and novel mutations may evade their detection. Together, these shortcomings urgently call for a reliable activity-based phenotypic assay.<sup>7,8</sup>

The only rapid phenotypic test for carbapenemase detection approved by Clinical & Laboratory Standards Institute (CLSI)

Received: January 14, 2021

Published: April 28, 2021



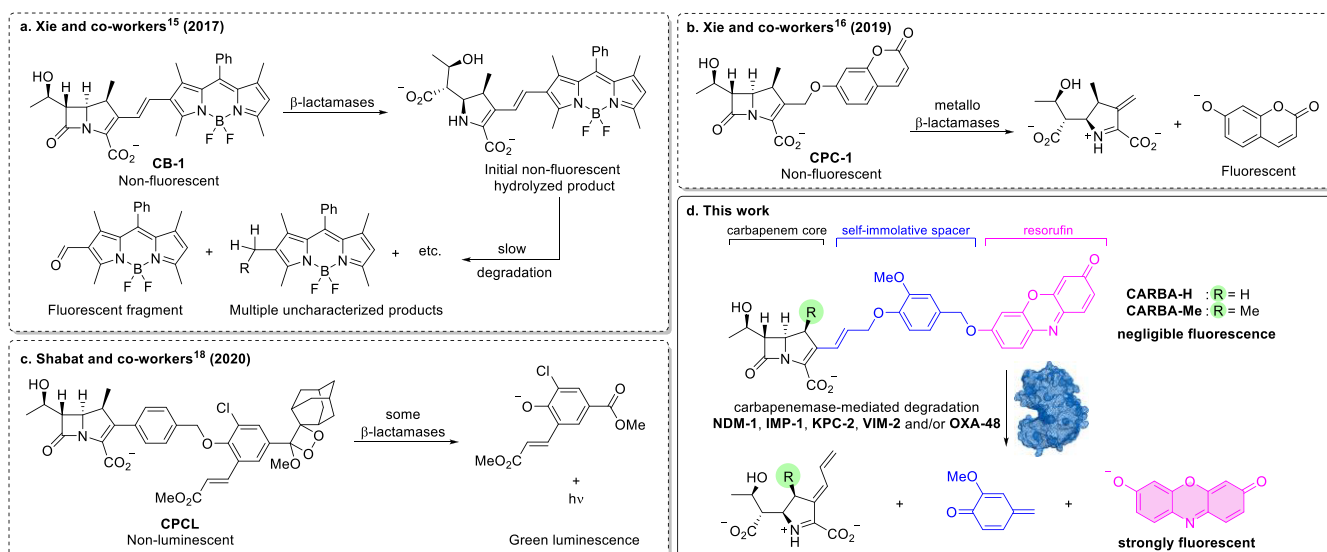


**Figure 1.** Previously reported carbapenem-based turn-on fluorogenic probes and the current design.

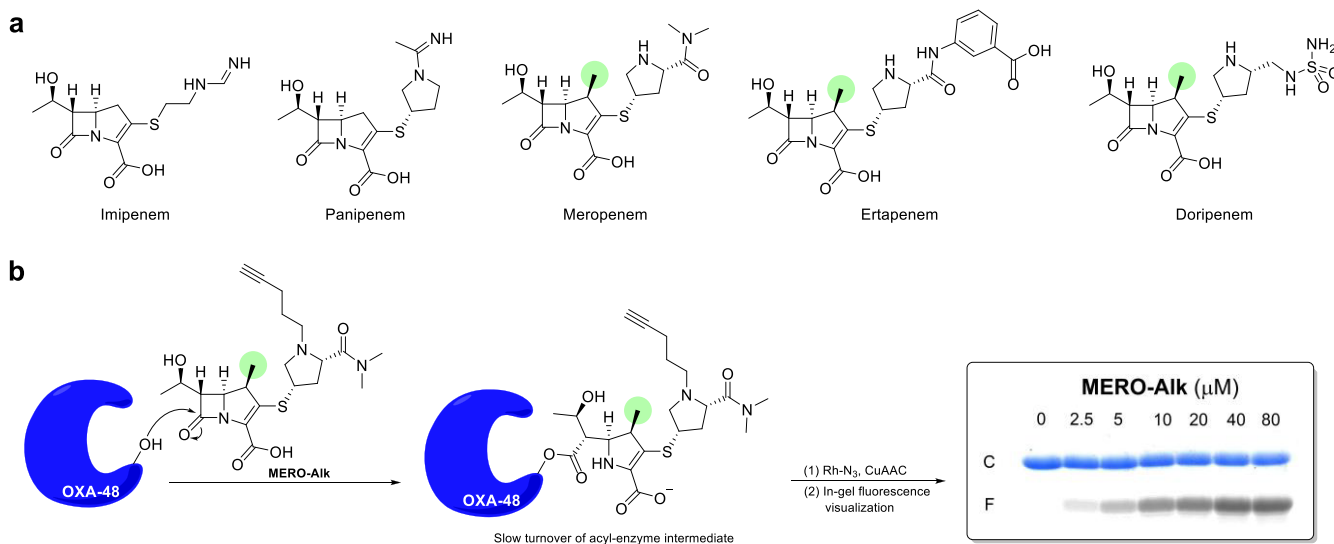


**Figure 2.** (a) Structures of some common carbapenem antibiotics. The  $1\beta$ -methyl substituent was highlighted with a green background. (b) Recombinant OXA-48 ( $5\ \mu\text{M}$ ) was incubated with **MERO-Aik** at different concentrations, followed by CuAAC and SDS-PAGE analysis. Coomassie blue staining was indicated with C and in-gel fluorescence visualization was indicated with F.

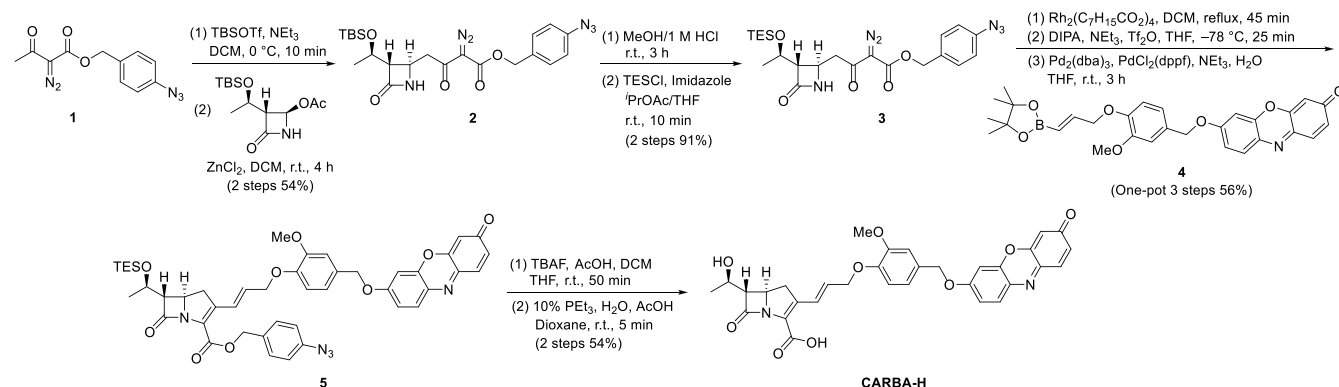
to date is CarbaNP.<sup>9,10</sup> While nominally it can offer a result in 2 h, the pH-based colorimetric assay is highly insensitive. Notably, false-negative results have been reported in the detection of OXA-48 (sensitivity as low as 11%) and enzymes possessing lower carbapenemase activities like SME and GES.<sup>7,9,10</sup> Indeterminate results can also arise due to the subtlety of the color difference, thus invalidating the test in those circumstances. Since its identification, OXA-48 has emerged as one of the most clinically important carbapenemases,<sup>11–14</sup> yet none of the existing chemical probes could address the challenge of its detection.<sup>9,10,15–19</sup> In addition, certain carbapenem-derived fluorescent probes reported in the literature only responded to particular classes of carbapenemases<sup>16</sup> (Figure 1a–c), underscoring the fact that careful consideration must be put into probe design in order to cover the entire range of carbapenemases. Noting the above shortcomings, we endeavor to design a fluorogenic substrate that selectively turns on toward a broad spectrum of

carbapenemases, encompassing the OXA-48-like carbapenemases in particular, and remains unresponsive toward non-carbapenemases.

## RESULTS AND DISCUSSION

**Hypothesis and Preliminary Observation.** The failure of OXA-48 detection by existing phenotypic tests points to a poor enzyme–substrate interaction, thus, we aimed to discover a molecular architecture that favors the binding and recognition. We noticed from the literature that OXA-48 exhibited at least 2 orders of magnitude higher catalytic efficiency ( $k_{\text{cat}}/K_{\text{M}}$ ) toward hydrolysis of imipenem and panipenem than that of meropenem, ertapenem, and doripenem.<sup>20,21</sup> Although these carbapenems bear different side chains, we recognized a dichotomous feature in which a  $1\beta$ -methyl substituent is present at the carbapenem core in the latter group but not in the former (Figure 2a). While the  $1\beta$ -methyl substituent is crucial for the suppression of hydrolytic

Scheme 1. Summary of Synthesis Toward CARBA-H



degradation of carbapenems by human peptidase DHP-1 in the renal brush border,<sup>22,23</sup> it may account for the failure of existing carbapenem-based sensors in detecting OXA-48. Meanwhile, Schofield and co-workers' molecular dynamic simulations provided *in silico* evidence that the 1 $\beta$ -methyl substituent in doripenem hindered the hydrolysis of the enzyme–substrate complex in OXA-1, a non-carbapenemase homologue of OXA-48.<sup>24</sup> We therefore hypothesized that the 1 $\beta$ -methyl substituent in carbapenems stabilizes the acyl-enzyme intermediate in OXA-48 and impedes the enzymatic turnover.

To provide experimental evidence, we prepared an alkyne-appended meropenem derivative, **MERO-Alk**, as a representative 1 $\beta$ -methyl bearing substrate for preliminary investigations (Figure 2b). If a stable covalent adduct is formed with OXA-48, the enzyme can be fluorescently labeled upon conjugation to an azido fluorophore using copper-catalyzed azide–alkyne cycloaddition (CuAAC). Accordingly, recombinant OXA-48 was incubated with different concentrations of **MERO-Alk** for 30 min, followed by treatment with rhodamine-azide (Rh–N<sub>3</sub>) under CuAAC conditions, and the results were evaluated using in-gel fluorescent visualization. In line with our hypothesis, an increase in fluorescence was observed in the presence of **MERO-Alk** in a dose dependent manner, suggesting that **MERO-Alk** forms a covalent adduct with OXA-48 (Figure 2b).

To validate whether the adduct formation preferentially takes place with 1 $\beta$ -methyl substituted carbapenems, we performed competition assays with meropenem and ertapenem (both bearing a 1 $\beta$ -methyl group) and imipenem (without 1 $\beta$ -methyl group). Recombinant OXA-48 was preincubated with the aforementioned carbapenems (30 min) before the addition of **MERO-Alk**. In-gel visualization showed that the fluorescence signal can be depleted by meropenem and ertapenem but not by imipenem, strongly indicating that the covalent modification took place in the enzyme active site selectively with carbapenems featuring a 1 $\beta$ -methyl group (Figure S1a–c). Analogous labeling experiments were conducted with a panel of purified recombinant carbapenemases which are clinically relevant. Neither carbapenemases from other classes (i.e., Classes A and B) nor heat-denatured OXA-48 but only catalytically active OXA-48 could be fluorescently tagged, consistent with the notion that the covalent modification corresponds to the formation of the acyl intermediate and is specific toward OXA-48 (Figure S1d).

We further confirmed the acylation indeed took place at the active site by a tandem mass spectrometry approach. OXA-48 was incubated with **MERO-Alk**, followed by CuAAC with a

commercially available acid-cleavable biotin-azide. The acylated OXA-48 was enriched by streptavidin–biotin enrichment followed by trypsin digestion. The modified peptide was cleaved and analyzed by LC-MS/MS, and the fragment search helped us identify that the modification took place in the active site (Figure S2). This mechanistic investigation uncovered a novel role of the 1 $\beta$ -methyl substituent in carbapenems and provided a rationale for our probe design.

In addition, we hope to integrate another structural feature in our design to achieve generality for pan-carbapenemase detection. It has been observed that the hydrolysis kinetics of certain  $\beta$ -lactamases are sensitive to substituent effects in the proximity of the  $\beta$ -lactam ring.<sup>16,25–27</sup> As different  $\beta$ -lactamases operate through different hydrolytic mechanisms, their active sites also exhibit significantly diverse structures.<sup>28</sup> Hence, we reasoned that by placing fluorophores, usually featuring extended  $\pi$ -systems that are electronically dissimilar to the polar side chains commonly found in carbapenems, further away from the core would allow probe recognition by a wider range of carbapenemases.

**Probe Design and Synthesis.** To this end, we aspired to construct our carbapenemase probes from three key building blocks, namely, a fluorogenic unit, a self-immolative spacer, and a carbapenem core. Resorufin was selected as the fluorogenic unit, as it not only demonstrates a strong turn-on fluorescence upon uncaging but also exhibits long excitation and emission wavelengths, which minimize undesired interference from autofluorescent biological molecules.<sup>29–31</sup> In addition, upon release, it also provides a colorimetric change that can be captured by naked eye, thus precluding the need of extra instrumentation. A self-immolative allylic-hydroxybenzylic linker was used to bridge the fluorogenic unit and the carbapenem core, which should steer the fluorogenic unit away from the core and enable a broader carbapenemase recognition. To pin down the role of the 1 $\beta$ -methyl group as a stereochemical determinant for the selectivity in OXA-48, we designed two target molecules, namely, **CARBA-H** and **CARBA-Me**, with and without the 1 $\beta$ -methyl substituent in the carbapenem core, respectively (Figure 1d).

A modular synthetic strategy was adopted (Scheme 1), which allows for flexibility in the installation of alternative chromophores if other emission wavelengths or detection approaches are desired. The linker-fluorophore fragment **4** was prepared from propargyl alcohol through an 8-step sequence that terminates with the attachment of resorufin (Scheme S1). For the carbapenem fragment, we adopted the azidobenzyl ester as a carboxylic acid protecting group.<sup>32,33</sup> It provides

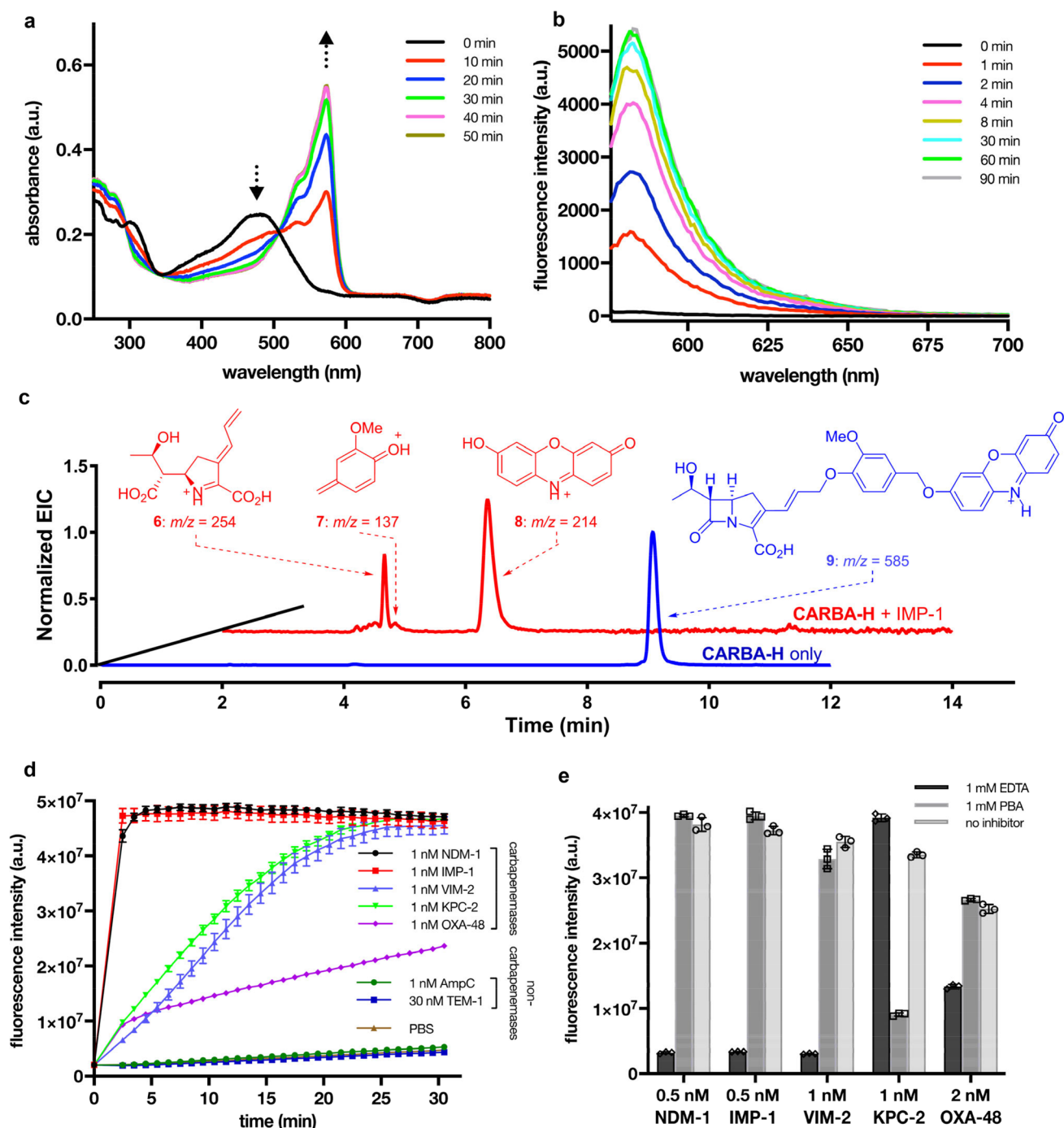


**Figure 3.** (a) Change in absorbance over time of CARBA-H ( $10 \mu\text{M}$  in PBS, pH 7.4) in the presence of IMP-1 (2 nM). (b) Fluorescence change over time of CARBA-H ( $1 \mu\text{M}$  in PBS, pH 7.4) toward IMP-1 (0.5 nM).  $\lambda_{\text{ex}} = 571 \text{ nm}$ . (c) Extracted ion chromatogram of HPLC-ESI MS analysis. CARBA-H ( $15 \mu\text{M}$ ) hydrolyzed by IMP-1 (10 nM) in  $\text{NH}_4\text{OAc}$  buffer (10 mM, pH 7.4), normalized to the largest peak. Observed peaks with selected mass-to-charge ratio ( $m/z$ ) corresponding to the expected fragments were indicated. (d) Fluorescence change over time of CARBA-H ( $2 \mu\text{M}$  in PBS, pH 7.4) toward selected  $\beta$ -lactamases.  $\lambda_{\text{ex}} = 564 \text{ nm}$ ;  $\lambda_{\text{em}} = 629 \text{ nm}$ . The error bars correspond to the standard deviation of the three replicates. (e) Fluorescence change of CARBA-H ( $2 \mu\text{M}$  in PBS, pH 7.4) in the presence of selected carbapenemases and  $\beta$ -lactamase inhibitors incubated for 30 min.  $\lambda_{\text{ex}} = 564 \text{ nm}$ ;  $\lambda_{\text{em}} = 629 \text{ nm}$ . The error bars correspond to the standard deviation of the three replicates.

orthogonality toward other protecting groups, tolerates a wide range of transformations, and can be readily removed by Staudinger reduction. For CARBA-H, a Lewis acid ( $\text{ZnCl}_2$ )-mediated Mannich reaction yielded azetidinone **2** as a single diastereomer. Subsequent protecting group manipulations afforded precursor **3**. After rhodium-catalyzed ring closure and subsequent derivatization of the ensuing ketone to a vinyl triflate, fragments **3** and **4** were united utilizing a late-stage

Suzuki coupling, catalyzed by a 1:1 mixture of  $\text{Pd}_2\text{dba}_3$  and  $\text{Pd}(\text{dppf})\text{Cl}_2$  under the optimized conditions to provide **5**. CARBA-H was successfully obtained upon global deprotection, and the control probe CARBA-Me was synthesized in an analogous fashion (Scheme S2).

**$\beta$ -Lactamase Response toward CARBA-H and CARBA-Me.** With the probes in hand, we first proceeded to measure the photophysical change of CARBA-H upon  $\beta$ -lactamase ring

opening by IMP-1, a typical carbapenemase. Over the course of reaction between CARBA-H (10  $\mu\text{M}$ ) and IMP-1 (2 nM), a decrease in absorbance at 480 nm was observed along with a simultaneous increase at 571 nm (Figure 3a). The new absorption maximum coincided with the reported value of resorufin.<sup>31</sup> A single isosbestic point at 507 nm implied that no intermediate was formed during the hydrolysis (Figure 3a). The presence of the expected fragmentation products was confirmed using HPLC-ESI MS (Figure 3c). Expectedly, the addition of IMP-1 resulted in the disappearance of signal corresponding to protonated CARBA-H (9), and the appearance of those corresponding to the protonated pyrrolidine 6, quinonemethide 7 and resorufin 8. For the fluorescence change, CARBA-H (1  $\mu\text{M}$ ) provided more than 60-fold fluorescence enhancement upon the addition of IMP-1 (0.5 nM) in only 8 min (Figure 3b). This compares very favorably with existing reports,<sup>10,15–18</sup> e.g., a much higher concentration (100 nM) of IMP-1 was required (cf. 0.5 nM IMP-1 for CARBA-H) to achieve a similar degree of enhancement with CB-1 under otherwise identical conditions.<sup>15</sup> The pseudo-first order rate constant for the spontaneous hydrolysis reaction (PBS, pH 7.4) of CARBA-H was estimated to be  $1.37 \times 10^{-5} \text{ s}^{-1}$  at room temperature, similar to that of carbapenems (Figure S3).<sup>16,19,34,35</sup>

We then evaluated the selectivity of the response of CARBA-H toward carbapenemases over other  $\beta$ -lactamases. Since NDM, IMP, VIM (Ambler Class B metallo- $\beta$ -lactamases), KPC (Class A serine carbapenemases), and OXA-48-like carbapenemases (Class D serine carbapenemases) account for more than 99% of the carbapenemase-producing isolates,<sup>36</sup> a representative member from each of these families, namely, NDM-1, IMP-1, VIM-2, KPC-2, and OXA-48, were recombinantly expressed, purified, and utilized in this study to examine the carbapenemase selectivity and coverage of our probes (Figure S4). Two common non-carbapenemases, AmpC (Class C serine  $\beta$ -lactamase) and TEM-1 (Class A serine  $\beta$ -lactamase), were employed as negative controls. The fluorescence change of CARBA-H (2  $\mu\text{M}$ ) toward the aforementioned enzymes (at 1 nM concentration except 30 nM for TEM-1) was monitored over 30 min (Figure 3d). CARBA-H only gave significant fluorescence enhancement in the presence of carbapenemases (i.e., NDM-1, IMP-1, VIM-2, KPC-2, and OXA-48), but not with non-carbapenemases (i.e., AmpC and TEM-1) over the period.

To validate that the response of CARBA-H was due to bona fide carbapenemase activity, we tested the effect of phenylboronic acid (PBA), a KPC-specific inhibitor, and ethylenediaminetetraacetic acid (EDTA), a metallo- $\beta$ -lactamase inhibitor, on the hydrolysis of CARBA-H by carbapenemases. In the presence of PBA, only KPC-2 activity was significantly blunted, and the enzymatic activities of NDM-1, IMP-1, VIM-2, and OXA-48 were not affected. Meanwhile, in the presence of EDTA, the activities of NDM-1, IMP-1, and VIM-2 were inhibited but remained unchanged for KPC-2 (Figure 3e). Interestingly, OXA-48 displayed a slightly decreased activity in the presence of EDTA, which is likely due to the increase in ion concentration.<sup>37</sup>

We also evaluated the performance of CARBA-Me against the same panel of carbapenemases (Figure S5). The fluorescence turn-on profiles for NDM-1, IMP-1, KPC-2, and VIM-2 were similar to that of CARBA-H; however, CARBA-Me did not yield a significant response toward OXA-48. While

the detection limits of CARBA-H and CARBA-Me toward each carbapenemase can be improved upon prolonged incubation, we chose a 30 min time frame for evaluation purposes as it represents a reasonable duration for a rapid test. The detection limits were in picomolar range for both probes toward VIM-2 and KPC-2, and in subpicomolar range for IMP-1 and NDM-1 (Table 1, Table S1, Figures S6, S7). To

**Table 1. Detection Limit (3S/k) of CARBA-H (2  $\mu\text{M}$  in PBS, pH 7.4) Toward Selected Carbapenemases Where S Is the Standard Deviation of 6 Blank Samples<sup>a</sup>**

Carbapenemase	3S/k
NDM-1	0.327 pM
IMP-1	0.333 pM
VIM-2	3.28 pM
KPC-2	4.43 pM
OXA-48	30.3 pM

<sup>a</sup> $\lambda_{\text{ex}} = 564 \text{ nm}$ ;  $\lambda_{\text{em}} = 629 \text{ nm}$ .

our delight, while OXA-48 led to the slowest turn-on fluorescence among all the carbapenemases, the corresponding value is still in the picomolar range.

To gain a better understanding of the substrate-enzyme interactions between CARBA-H/CARBA-Me and our panel of carbapenemases, the Michaelis–Menten kinetics model was adopted. Our enzyme kinetics data showed that CARBA-H served as an excellent substrate for carbapenemases, explaining the rapid turn-on response (Table 2, Figure S8). For VIM-2,

**Table 2. Michaelis–Menten Kinetics Data<sup>a</sup>**

enzyme	$k_{\text{cat}}$ ( $\text{s}^{-1}$ )	$K_{\text{M}}$ ( $\mu\text{M}$ )	$k_{\text{cat}}/K_{\text{M}}$ ( $\text{M}^{-1} \text{ s}^{-1}$ )
NDM-1	$29.78 \pm 0.81$	$1.66 \pm 0.13$	$1.80 \times 10^7$
IMP-1	$33.86 \pm 0.71$	$1.20 \pm 0.08$	$2.82 \times 10^7$
VIM-2	$1.96 \pm 0.05$	$1.18 \pm 0.10$	$1.66 \times 10^6$
KPC-2	$2.17 \pm 0.07$	$0.93 \pm 0.11$	$2.32 \times 10^6$
OXA-48	$2.83 \pm 0.18$	$0.66 \pm 0.08$	$4.25 \times 10^6$

<sup>a</sup> $k_{\text{cat}}$  and  $K_{\text{M}}$  values for CARBA-H.

KPC-2, and OXA-48, the turnover numbers ( $k_{\text{cat}}/K_{\text{M}}$ ) were found to be in the order of  $10^6 \text{ M}^{-1} \text{ s}^{-1}$ , while those of NDM-1 and IMP-1 were even in the order of  $10^7 \text{ M}^{-1} \text{ s}^{-1}$ . In general, the  $k_{\text{cat}}/K_{\text{M}}$  values for NDM-1, IMP-1, VIM-2, and KPC-2 toward CARBA-H and CARBA-Me are similar to that with imipenem and meropenem (Table 2, Table S2, Figure S9).<sup>38–42</sup> However, the corresponding values for the reaction between OXA-48 and CARBA-Me could not be determined, as the initial hydrolysis rate of CARBA-Me was found to be independent of OXA-48 concentration. The observation is again consistent with our preliminary protein labeling study in which 1 $\beta$ -methyl bearing substrates form a relatively stable acyl intermediate with OXA-48, thus rendering the Michaelis–Menten model unsuitable for the analysis.

**Rapid Test Assays with Clinical Isolates.** Encouraged by the results, we proceeded to apply CARBA-H to detect carbapenemase activities in clinical isolates of *Klebsiella pneumoniae*, *Escherichia coli*, *Enterobacter aerogenes* (*Klebsiella aerogenes*), and *Citrobacter freundii*, which represent the most clinically relevant families of carbapenem-resistant Enterobacteriaceae.<sup>1</sup> Thirteen carbapenemase-encoding strains were used as positive controls (Figure 4). In addition to producers of KPC-2 (strain 1) and NDM-1 (strain 2), of which

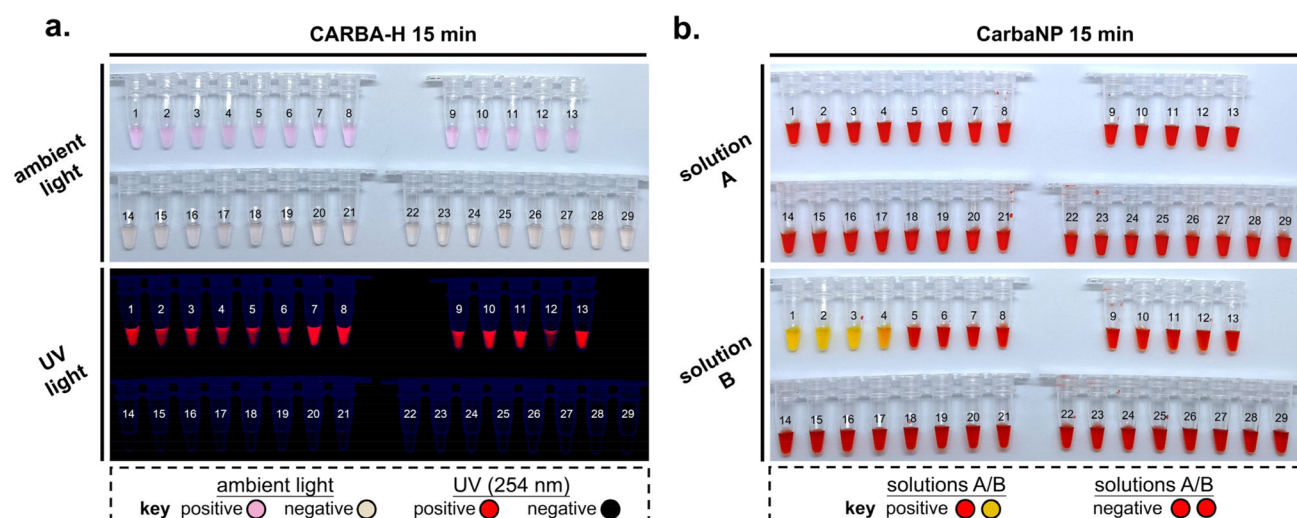


**Figure 4.** (a) Colorimetric and fluorogenic (UV 254 nm) response of **CARBA-H** (10  $\mu\text{M}$ ) (b) CarbaNP solution A and solution B, toward clinical isolates according to CLSI protocol. Images were taken after incubation for 15 min. The carbapenemases encoded in the clinical isolates were determined by PCR. Strain (1) *K. pneumoniae* (KPC-2); (2) *E. coli* (NDM-1); (3) *E. coli* (NDM-5); (4) *E. coli* (IMP-4); (5) *E. coli* (OXA-181); (6) *E. coli* (OXA-181); (7) *K. pneumoniae* (OXA-181); (8) *K. pneumoniae* (OXA-181); (9) *E. coli* (OXA-48); (10) *E. aerogenes* (OXA-48); (11) *E. aerogenes* (OXA-48); (12) *C. freundii* (OXA-48); (13) *K. pneumoniae* (OXA-48); (14–21) *K. pneumoniae* (non-CPE); (22–29) *E. coli* (non-CPE).

the enzymatic activities toward **CARBA-H** were carefully characterized, we included strains that produce NDM-5 (strain 3) and IMP-4 (strain 4), homologues of NDM-1 and IMP-1, respectively, to demonstrate the pan-carbapenemase coverage of our probe. Moreover, 9 strains (from 4 different organisms) that express OXA-181 (strains 5–8) and OXA-48 (strains 9–13) were employed to showcase the unique ability of **CARBA-H** to detect the OXA-48-like family. The presence of the carbapenemase-encoding genes in these isolates were cross validated by PCR, and 16 non-carbapenemase-producing Enterobacteriaceae (non-CPE) isolates (strains 14–29) were used as negative controls.

While the detection can be carried out with live bacteria as carbapenemases are often secreted (Figure S10a), we sought to lyse the bacteria in order to release the carbapenemases from the periplasmic space of the bacteria for rapid detection purposes. We first investigated the efficiency of some nondenaturing detergents, namely Triton X-100, Tween-20, 3-[(3-cholamidopropyl)-dimethylammonio]-1-propanesulfonate (CHAPS), and B-PER, as additives in PBS buffer. Accordingly, bacteria were incubated with **CARBA-H** in the detergent-containing buffer solutions, and the efficiency of bacterial lysis was determined by the degree of color change after 15 min (Figure S10b–S11). CHAPS was found to provide the most rapid color change and hence was selected for the subsequent rapid test assay. Thus, clinical isolates were lysed in PBS buffer containing 0.5% CHAPS for 15 min before **CARBA-H** treatment (Figure S12). The carbapenemase-encoding strains (Figure 4a; strains 1–13) induced marked color change from pale orange to deep pink, visible under ambient light, within 15 min. In contrast, the color of the negative controls remained unchanged (Figure 4a; strains 14–29). The fluorescence turn-on could also be conveniently visualized with the aid of a hand-held UV lamp. Again, only the CPE strains provided intense fluorescence signals (Figure 4a; strains 1–13 vs 14–29). A consistent observation was obtained after prolonged incubation (120 min; Figure S13a), indicating the fluorescent probe and fluorophore are stable in the complex biological system as a reliable rapid test. A head-to-

head comparison was made by performing the CarbaNP test in parallel. In contrast to **CARBA-H**, CarbaNP did not provide any positive color change for the bacteria expressing Class D carbapenemases (strains 9–13) within 15 min (Figure 4a). Even with prolonged incubation for up to 120 min, the maximum incubation time as recommended by CLSI for CarbaNP, CarbaNP did not provide a distinct color change, corresponding to false-negative or inconclusive results for those isolates (Figure S13c). Moreover, due to the high sensitivity, even OXA-232, a known Class D carbapenemase with notably low carbapenemase activity, can be clearly detected (Figure S13a, strains 30–32). For completeness, a direct comparison against **CARBA-Me** was also performed (Figure S13b). As expected, after 120 min, **CARBA-Me** provided the colorimetric and fluorogenic responses toward KPC, NDM, and IMP-encoding strains but variable results toward the strains encoding the OXA-48-like carbapenemases. Together, our study clearly showcased the superior performance of **CARBA-H** over existing protocols and probe designs.

**Urine Test with Clinical Isolates.** To demonstrate potential clinical applicability of **CARBA-H**, we set out to detect carbapenemase activity directly in urine samples. Urinary tract infection (UTI) was reported to be leading healthcare-associated infection among hospitalized adults and in critical care units, and the second or third most common type of nosocomial infection in intensive care units.<sup>43,44</sup> As a proof of concept, we mimicked urine samples from UTI patients by spiking urine from healthy subjects with known amounts of well-characterized carbapenemase-producing clinical isolates, particularly with the inclusion of OXA-48, OXA-181, and OXA-232-producing strains. Remarkably, **CARBA-H** (0.25  $\mu\text{M}$ ) provided significant fluorescence enhancement in all CPE-spiked ( $5 \times 10^6$  cfu) urine samples, in the presence of 0.5% CHAPS, within 2 h. The turn-on response could be readily detected by a microplate reader, with a clear differentiation against the background from non-CPE *E. coli* and *K. pneumoniae* isolates (Figure 5). This assay potentially obviates the need for bacterial culture and creates new opportunities for rapid detection of UTI by CRE, as the

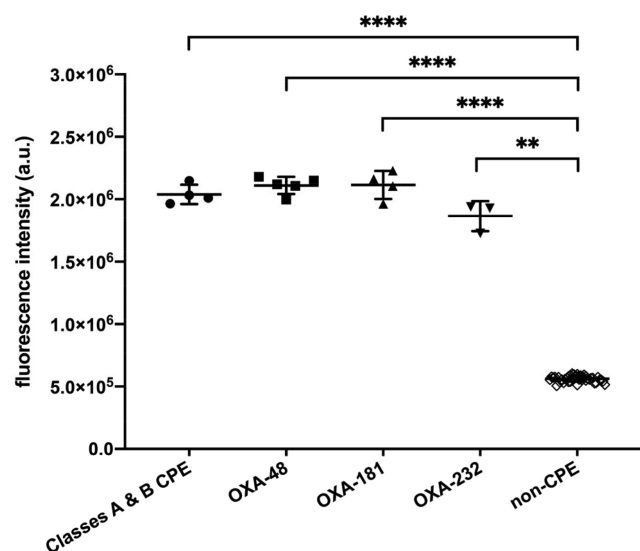


**Figure 5.** Fluorescent response of CARBA-H (0.25  $\mu\text{M}$ ;  $\lambda_{\text{ex}} = 564$  nm;  $\lambda_{\text{em}} = 629$  nm) toward carbapenemase in a panel of 71 Enterobacteriaceae clinical isolates spiked in urine ( $5 \times 10^6$  cfu), was determined upon incubation at 37  $^{\circ}\text{C}$  for 2 h. Strain (1) *E. coli* (IMP-4); (2) *K. pneumoniae* (KPC-2); (3) *E. coli* (NDM-1); (4) *E. coli* (NDM-5); (5) *C. freundii* (OXA-48); (6) *E. aerogenes* (OXA-48); (7) *E. aerogenes* (OXA-48); (8) *E. coli* (OXA-48); (9) *K. pneumoniae* (OXA-48); (10) *E. coli* (OXA-181); (11) *E. coli* (OXA-181); (12) *K. pneumoniae* (OXA-181); (13) *K. pneumoniae* (OXA-181); (14) *E. coli* (OXA-232); (15) *K. pneumoniae* (OXA-232); (16) *K. pneumoniae* (OXA-232); (17–24) *K. pneumoniae* (non-CPE); (25–71) *E. coli* (non-CPE). The error bars correspond to the standard deviation of the two replicates. Statistical significance was calculated using the unpaired two-tailed Student's *t* test with Welch's correction (\*\*  $p < 0.01$ , \*\*\*\*  $p < 0.0001$ ).

necessary bacterial count is readily achievable by routine centrifugation of patient urine samples as per traditional urinalysis<sup>45</sup> (typical UTI patients are reported to have a bacterial count exceeding  $1 \times 10^5$  cfu/mL in their urine).<sup>44,46</sup> This could further reduce the time for culturing bacteria and minimize delay for the golden treatment period. The compatibility of the fluorogenic carbapenemase detection using CARBA-H in urine samples highlights the judicious choice of the reporting fluorophore (Figure S14) and demonstrates the scope for extending this strategy for use in other biological specimens.

## DISCUSSION

The success in the development of CARBA-H as a fluorescent probe for broad spectrum carbapenemase detection hinges upon our rational design with two key features, i.e., an effective self-immolative spacer and the lack of the  $1\beta$ -methyl substituent at the carbapenem core.

The allylic-hydroxybenzyl self-immolative spacer in our probe design is crucial in providing high sensitivity and a broad scope for carbapenemase detection. A CARBA-H analog without the self-immolative spacer was also prepared as a control (Figure S15 and Scheme S3). As expected, the molecule displayed poor response toward KPC-2 and suffered from poor aqueous stability. At the outset of the project, we also briefly explored the use of a phenyl spacer, which was later found to be utilized in a recent carbapenem-based probe design.<sup>18</sup> However, this strategy resulted in incomplete fluorophore release during carbapenemase mediated hydrolysis

(Figures S16 and Scheme S4), leading to a drastic decrease in sensitivity. In contrast, the small allylic spacer in CARBA-H and CARBA-Me provided a complete and immediate fluorophore uncaging upon carbapenem ring opening (Figure S17), resulting in maximum chromophore release suited for rapid detection. This highlights that, in the context of small molecule-based chemosensors, extra consideration should be made in linker selection for future probe design to maximize signal generation.

Through a chemical biology approach, we have uncovered a crucial role of  $1\beta$ -methyl group in carbapenems during OXA-48 mediated hydrolysis. Recent reports by Chen<sup>47</sup> and Vakulenko<sup>48</sup> on crystal structures of OXA-48 and its covalent adducts with several carbapenems shed light on the enzymatic mechanisms, yet these structural studies could not offer ready explanation for the slow hydrolysis kinetics with  $1\beta$ -methyl substituted carbapenems.<sup>49</sup> Meanwhile, Schofield and co-workers showed that the presence of  $1\beta$ -methyl group led to a detour in the carbapenem degradation pathway with OXA-48.<sup>24</sup> In this study, we revealed that this substituent is crucial in slowing down the deacylation process, and this discovery provides new insight for antibiotic therapy and drug discovery. Clinical research has shown that patient infected with certain carbapenemase-producing bacteria (e.g., OXA-48-encoding bacteria) could be effectively treated with coadministration of two carbapenem antibiotics (i.e., double-carbapenem therapy).<sup>50,51</sup> To explain the observed synergistic effect, we postulated that one of the carbapenems act as a suicidal inhibitor for OXA-48, and the other targets the bacterial cell wall synthesis.<sup>50,51</sup> While there is almost no molecular evidence to back up such treatment, our finding provided strong rationale for this therapy from a mechanistic perspective.

## CONCLUSION

We have developed CARBA-H successfully as the first broad spectrum off-on fluorogenic carbapenemase probe. Through direct comparison on the performance of CARBA-H with CARBA-Me and a series of mechanistic studies, we have provided clear evidence that the  $1\beta$ -methyl substituent strongly affects the OXA-48 enzyme hydrolytic kinetics. CARBA-H exhibit excellent sensitivity toward the 5 clinically most relevant carbapenemases, including OXA-48, of which the detection limit was determined to be in the pico-molar range.

We have applied our probe CARBA-H to an optimized rapid test for carbapenemase detection in clinical isolates. The absence of the  $1\beta$ -methyl substituent is essential for pan-carbapenemase recognition, where carbapenemase encoding strains, including OXA-48, OXA-181, and OXA-232, could be successfully detected. Reliable chromogenic and fluorogenic readouts could be easily discerned by naked eye within 15 min, demonstrating its outstanding performances compared to currently existing assays. Our success in establishing an operationally simple protocol for detecting carbapenemase activities from clinical isolates should accelerate the development of an affordable point-of-care device, for antimicrobial resistance tests performed without specialized equipment available only in hospitals.

## ASSOCIATED CONTENT

### Supporting Information

The Supporting Information is available free of charge at <https://pubs.acs.org/doi/10.1021/jacs.1c00462>.

(PDF)

## ■ AUTHOR INFORMATION

## Corresponding Author

Dan Yang – Morningside Laboratory for Chemical Biology, Department of Chemistry, The University of Hong Kong, Hong Kong, China; [orcid.org/0000-0002-1726-9335](https://orcid.org/0000-0002-1726-9335); Email: [yangdan@hku.hk](mailto:yangdan@hku.hk)

## Authors

Chi-Wang Ma – Morningside Laboratory for Chemical Biology, Department of Chemistry, The University of Hong Kong, Hong Kong, China; [orcid.org/0000-0002-6785-5148](https://orcid.org/0000-0002-6785-5148)

Kenneth King-Hei Ng – Morningside Laboratory for Chemical Biology, Department of Chemistry, The University of Hong Kong, Hong Kong, China

Bill Hin-Cheung Yam – Department of Microbiology and Carol Yu Centre for Infection, The University of Hong Kong, Hong Kong, China

Pak-Leung Ho – Department of Microbiology and Carol Yu Centre for Infection, The University of Hong Kong, Hong Kong, China; [orcid.org/0000-0002-8811-1308](https://orcid.org/0000-0002-8811-1308)

Richard Yi-Tsun Kao – Department of Microbiology and Carol Yu Centre for Infection, The University of Hong Kong, Hong Kong, China

Complete contact information is available at:

<https://pubs.acs.org/10.1021/jacs.1c00462>

## Notes

The authors declare the following competing financial interest(s): The results reported in this manuscript were included in a PCT Application (No. PCT/CN2019/106645) filed by D.Y. and C.-W.M.

## ■ ACKNOWLEDGMENTS

We acknowledge support from The University of Hong Kong, Morningside Foundation, small equipment grant (2019/20), the Hong Kong Research Grants Council under the General Research Fund Scheme (106200223), Areas of Excellence Scheme (AoE/P-705/16), and Health and Medical Research Fund (CID-HKU1-13).

## ■ REFERENCES

- (1) CDC Antibiotic Resistance Threats in the United States, 2019. Department of Health and Human Services, CDC. Atlanta, GA:U.S.: 2019.
- (2) Bush, K. Past and Present Perspectives on  $\beta$ -Lactamases. *Antimicrob. Agents Chemother.* **2018**, *62*, e01076–18.
- (3) Davies, J.; Davies, D. Origins and evolution of antibiotic resistance. *Microbiol. Mol. Biol. Rev.* **2010**, *74*, 417–33.
- (4) Funk, D. J.; Kumar, A. Antimicrobial therapy for life-threatening infections: speed is life. *Crit. Care Clin.* **2011**, *27*, 53–76.
- (5) Ibrahim, E. H.; Sherman, G.; Ward, S.; Fraser, V. J.; Kollef, M. H. The Influence of Inadequate Antimicrobial Treatment of Bloodstream Infections on Patient Outcomes in the ICU Setting. *Chest* **2000**, *118*, 146–155.
- (6) Meunier, D.; Freeman, R.; Hopkins, K. L.; Hopkins, S.; Woodford, N.; Brown, C.; Chilton, C.; Davies, F.; Davies, K.; Lewis, T.; Otter, J.; Richards, D.; Soyfoo, R.; Wilcox, M. *Commercial assays for the detection of acquired carbapenemases*; Public Health England: 2019.
- (7) Hindler, J. A.; Schuetz, A. N.; Abbott, A.; Antonara, S.; Bobenchik, A.; Castanheira, M.; Charnot-Katsikas, A.; Galas, M.;

Humphries, R.; Rekasius, V.; Scangarella-Oman, N.; Westblade, L. *CLSI AST News Update* **2017**, *2*, 1–17.

(8) Hemarajata, P.; Yang, S.; Hindler, J. A.; Humphries, R. M. Development of a novel real-time PCR assay with high-resolution melt analysis to detect and differentiate OXA-48-Like  $\beta$ -lactamases in carbapenem-resistant Enterobacteriaceae. *Antimicrob. Agents Chemother.* **2015**, *59*, 5574–80.

(9) Tamma, P. D.; S, P. J. Phenotypic Detection of Carbapenemase-Producing Organisms from Clinical Isolates. *J. Clin. Microbiol.* **2018**, *56*, e01140–18.

(10) *CLSI Performance Standards for Antimicrobial Susceptibility Testing*, 29th ed.; Clinical and Laboratory Institute: Wayne, PA 2019.

(11) Pitout, J. D. D.; Peirano, G.; Kock, M. M.; Strydom, K. A.; Matsumura, Y. The Global Ascendency of OXA-48-Type Carbapenemases. *Clin. Microbiol. Rev.* **2019**, *33*, e00102–19.

(12) Hernandez-Garcia, M.; Perez-Viso, B.; Navarro-San Francisco, C.; Baquero, F.; Morosini, M. I.; Ruiz-Garbajosa, P.; Canton, R. Intestinal co-colonization with different carbapenemase-producing Enterobacteriales isolates is not a rare event in an OXA-48 endemic area. *EclinicalMedicine* **2019**, *15*, 72–79.

(13) Branas, P.; Gil, M.; Villa, J.; Orellana, M. A.; Chaves, F. Molecular epidemiology of carbapenemase-producing Enterobacteriaceae infection/colonisation in a hospital in Madrid. *Enferm. Infecc. Microbiol. Clin.* **2018**, *36*, 100–103.

(14) Cui, X.; Zhang, H.; Du, H. Carbapenemases in Enterobacteriaceae: Detection and Antimicrobial Therapy. *Front. Microbiol.* **2019**, *10*, 1823.

(15) Mao, W.; Xia, L.; Xie, H. Detection of Carbapenemase-Producing Organisms with a Carbapenem-Based Fluorogenic Probe. *Angew. Chem., Int. Ed.* **2017**, *56*, 4468–4472.

(16) Mao, W.; Wang, Y.; Qian, X.; Xia, L.; Xie, H. A Carbapenem-Based Off-On Fluorescent Probe for Specific Detection of Metallo- $\beta$ -Lactamase Activities. *ChemBioChem* **2019**, *20*, 511–515.

(17) Kim, J.; Kim, Y.; Abdelazem, A. Z.; Kim, H. J.; Choo, H.; Kim, H. S.; Kim, J. O.; Park, Y. J.; Min, S. J. Development of carbapenem-based fluorogenic probes for the clinical screening of carbapenemase-producing bacteria. *Bioorg. Chem.* **2020**, *94*, 103405.

(18) Das, S.; Ihssen, J.; Wick, L.; Spitz, U.; Shabat, D. Chemiluminescence Carbapenem-based Molecular Probe for Detection of Carbapenemase Activity in Live Bacteria. *Chem. - Eur. J.* **2020**, *26*, 3647.

(19) Wang, J.; Xu, W.; Xue, S.; Yu, T.; Xie, H. A minor structure modification serendipitously leads to a highly carbapenemase-specific fluorogenic probe. *Org. Biomol. Chem.* **2020**, *18*, 4029–4033.

(20) Docquier, J. D.; Calderone, V.; De Luca, F.; Benvenuti, M.; Giuliani, F.; Bellucci, L.; Tafi, A.; Nordmann, P.; Botta, M.; Rossolini, G. M.; Mangani, S. Crystal structure of the OXA-48  $\beta$ -lactamase reveals mechanistic diversity among class D carbapenemases. *Chem. Biol.* **2009**, *16*, 540–7.

(21) Papp-Wallace, K. M.; Kumar, V.; Zeiser, E. T.; Becka, S. A.; van den Akker, F. Structural Analysis of The OXA-48 Carbapenemase Bound to A "Poor" Carbapenem Substrate, Doripenem. *Antibiotics* **2019**, *8*, 145–158.

(22) El-Gamal, M. I.; Brahim, I.; Hisham, N.; Aladdin, R.; Mohammed, H.; Bahaeldin, A. Recent updates of carbapenem antibiotics. *Eur. J. Med. Chem.* **2017**, *131*, 185–195.

(23) Fukasawa, M.; Sumita, Y.; Harabe, E. T.; Tanio, T.; Nouda, H.; Kohzaki, T.; Okuda, T.; Matsumura, H.; Sunagawa, M. Stability of meropenem and Effect of 1 $\beta$ -Methyl Substitution on Its Stability in the Presence of Renal Dehydropeptidase I. *Antimicrob. Agents Chemother.* **1992**, *7*, 1577–1579.

(24) Lohans, C. T.; van Groesen, E.; Kumar, K.; Tooke, C. L.; Spencer, J.; Paton, R. S.; Brem, J.; Schofield, C. J. A New Mechanism for  $\beta$ -Lactamases: Class D Enzymes Degrade 1 $\beta$ -Methyl Carbapenems through Lactone Formation. *Angew. Chem., Int. Ed.* **2018**, *57*, 1282–1285.

(25) Palzkill, T. Structural and Mechanistic Basis for Extended-Spectrum Drug-Resistance Mutations in Altering the Specificity of TEM, CTX-M, and KPC  $\beta$ -lactamases. *Front. Mol. Biosci.* **2018**, *5*, 16.



- (26) Neu, H. C.  $\beta$ -Lactam Antibiotics: Structural Relationships Affecting in Vitro Activity and Pharmacologic Properties. *Clin. Infect. Dis.* **1986**, *8*, S237–S259.
- (27) Romero, A.; Bou, G. N.; Beceiro, A.; Santillana, E. Crystal structure of the carbapenemase OXA-24 reveals insights into the mechanism of carbapenem hydrolysis. *Proc. Natl. Acad. Sci. U. S. A.* **2007**, *104*, 5354–5359.
- (28) Tooke, C. L.; Hinchliffe, P.; Bragginton, E. C.; Colenso, C. K.; Hirvonen, V. H. A.; Takebayashi, Y.; Spencer, J.  $\beta$ -Lactamases and  $\beta$ -Lactamase Inhibitors in the 21st Century. *J. Mol. Biol.* **2019**, *431*, 3472–3500.
- (29) Chan, J.; Dodani, S. C.; Chang, C. J. Reaction-based small-molecule fluorescent probes for chemoselective bioimaging. *Nat. Chem.* **2012**, *4*, 973–84.
- (30) Islam, M. S.; Honma, M.; Nakabayashi, T.; Kinjo, M.; Ohta, N. pH dependence of the fluorescence lifetime of FAD in solution and in cells. *Int. J. Mol. Sci.* **2013**, *14*, 1952–63.
- (31) Bueno, C.; Villegas, M. L.; Bertolotti, S. G.; Previtali, C. M.; Neumann, M. G.; Encinas, M. V. The Excited-State Interaction of Resazurin and Resorufin with Amines in Aqueous Solutions. *Photochem. Photobiol.* **2002**, *76*, 385–390.
- (32) Wang, J.; Chen, Y.; Yang, C.; Wei, T.; Han, Y.; Xia, M. An ICT-based colorimetric and ratiometric fluorescent probe for hydrogen sulfide and its application in live cell imaging. *RSC Adv.* **2016**, *6*, 33031–33035.
- (33) Griffin, R. J.; Evers, E.; Davison, R.; Gibson, A. E.; Layton, D.; Irwin, W. J. The 4-azidobenzoyloxycarbonyl function; application as a novel protecting group and potential prodrug modification for amines. *J. Chem. Soc., Perkin Trans. 1* **1996**, 1205–1211.
- (34) Dailly, E.; Bouquie, R.; Deslandes, G.; Jolliet, P.; Le Floch, R. A liquid chromatography assay for a quantification of doripenem, ertapenem, imipenem, meropenem concentrations in human plasma: application to a clinical pharmacokinetic study. *J. Chromatogr. B: Anal. Technol. Biomed. Life Sci.* **2011**, *879*, 1137–42.
- (35) Viaene, E.; Chanteux, H.; Servais, H.; Mingeot-Leclercq, M. P.; Tulkens, P. M. Comparative stability studies of antipseudomonal  $\beta$ -lactams for potential administration through portable elastomeric pumps (home therapy for cystic fibrosis patients) and motor-operated syringes (intensive care units). *Antimicrob. Agents Chemother.* **2002**, *46*, 2327–32.
- (36) English Surveillance Programme for Antimicrobial Utilisation and Resistance (ESPAUR). Public Health England, London, 2018.
- (37) Stojanoski, V.; Chow, D. C.; Fryszczyn, B.; Hu, L.; Nordmann, P.; Poirel, L.; Sankaran, B.; Prasad, B. V.; Palzkill, T. Structural Basis for Different Substrate Profiles of Two Closely Related Class D  $\beta$ -Lactamases and Their Inhibition by Halogens. *Biochemistry* **2015**, *54*, 3370–80.
- (38) Docquier, J. D.; Riccio, M. L.; Mugnaioli, C.; Luzzaro, F.; Endimiani, A.; Toniolo, A.; Amicosante, G.; Rossolini, G. M. IMP-12, a new plasmid-encoded metallo- $\beta$ -lactamase from a *Pseudomonas putida* clinical isolate. *Antimicrob. Agents Chemother.* **2003**, *47*, 1522–8.
- (39) Poirel, L.; Heritier, C.; Tolun, V.; Nordmann, P. Emergence of oxacillinase-mediated resistance to imipenem in *Klebsiella pneumoniae*. *Antimicrob. Agents Chemother.* **2004**, *48*, 15–22.
- (40) Alba, J.; Ishii, Y.; Thomson, K.; Moland, E. S.; Yamaguchi, K. Kinetics study of KPC-3, a plasmid-encoded class A carbapenem-hydrolyzing  $\beta$ -lactamase. *Antimicrob. Agents Chemother.* **2005**, *49*, 4760–2.
- (41) Piccirilli, A.; Brisdelli, F.; Aschi, M.; Celenza, G.; Amicosante, G.; Perilli, M. Kinetic Profile and Molecular Dynamic Studies Show that Y229W Substitution in an NDM-1/L209F Variant Restores the Hydrolytic Activity of the Enzyme toward Penicillins, Cephalosporins, and Carbapenems. *Antimicrob. Agents Chemother.* **2019**, *63*, e02270–18.
- (42) Docquier, J. D.; Lamotte-Brasseur, J.; Galleni, M.; Amicosante, G.; Frere, J. M.; Rossolini, G. M. On functional and structural heterogeneity of VIM-type metallo- $\beta$ -lactamases. *J. Antimicrob. Chemother.* **2003**, *51*, 257–66.
- (43) Suay-Garcia, B.; Perez-Gracia, M. T. Present and Future of Carbapenem-resistant Enterobacteriaceae (CRE) Infections. *Antibiotics* **2019**, *8*, 122.
- (44) Chan, J. F.-W.; Yuen, K.-Y. A new ASPECT for complicated urinary tract infections. *Lancet* **2015**, *385*, 1920–1922.
- (45) Wilson, M. L.; Gaido, L. Laboratory Diagnosis of Urinary Tract Infections in Adult Patients. *Clin. Infect. Dis.* **2004**, *38*, 1150–1158.
- (46) Foxman, B. The epidemiology of urinary tract infection. *Nat. Rev. Urol.* **2010**, *7*, 653–60.
- (47) Smith, C. A.; Stewart, N. K.; Toth, M.; Vakulenkob, S. B. Structural Insights into the Mechanism of Carbapenemase Activity of the OXA-48  $\beta$ -Lactamase. *Antimicrob. Agents Chemother.* **2019**, *63*, e01202–19.
- (48) Akhtar, A.; Pemberton, O. A.; Chen, Y. Structural Basis for Substrate Specificity and Carbapenemase Activity of OXA-48 Class D  $\beta$ -Lactamase. *ACS Infect. Dis.* **2020**, *6*, 261–271.
- (49) Stojanoski, V.; Hu, L.; Sankaran, B.; Wang, F.; Tao, P.; Prasad, B. V. V.; Palzkill, T. Mechanistic Basis of OXA-48-like  $\beta$ -Lactamases' Hydrolysis of Carbapenems. *ACS Infect. Dis.* **2021**, *7*, 445–460.
- (50) Galani, I.; Nafplioti, K.; Chatzikonstantinou, M.; Souli, M. In vitro evaluation of double-carbapenem combinations against OXA-48-producing *Klebsiella pneumoniae* isolates using time-kill studies. *J. Med. Microbiol.* **2018**, *67*, 662–668.
- (51) Mashni, O.; Nazer, L.; Le, J. Critical Review of Double-Carbapenem Therapy for the Treatment of Carbapenemase-Producing *Klebsiella pneumoniae*. *Ann. Pharmacother.* **2019**, *53*, 70–81.